Research Square

Preprints are preliminary reports that have not undergone peer review.
They should not be considered conclusive, used to inform clinical practice,
or referenced by the media as validated information.

Ionospheric scintillation climatology over Ethiopiaduring the rising phase of Solar Cycle 24

Tesfay Yemane Tesfu

tesfayphysics@gmail.com

Mekelle University College of Natural and Computational Sciences https://orcid.org/0000-0003-3833-1836

Luca Spogli

INGV: Istituto Nazionale di Geofisica e Vulcanologia

Gebregiorgis Abraha

Mekelle University College of Natural and Computational Sciences

Gizaw Mengistu Tsidu

Botswana International University of Science and Technology

Nat Gopalswamy

NASA Goddard Space Flight Center

Seiji Yashiro

NASA Goddard Space Flight Center

Research Article

Keywords:

Posted Date: November 25th, 2026

DOI: https://doi.org/10.21203/rs.3.rs-11618515/v1

License: This work is licensed under a Creative Commons Attribution 4.0 International License.
Read Full License

Ionospheric scintillation climatology over Ethiopia during the rising phase of Solar Cycle 24

Tesfay Yemane Tesfu[1,5,6*], Luca Spogli[4], Gebregiorgis Abraha Fikade[6], Gizaw Mengistu Tsidu[2,3], Nat Gopalswamy[5,6], Seiji Yashiro[5]

[1]Department of Physics, Mekelle University, Mekelle, Tigray, Ethiopia.
[2]Department of Physics, Addis Ababa University, Addis Ababa, Ethiopia.
[3]Department of Earth and Environmental Sciences, College of Science, Botswana International University of Science and Technology (BIUST), Private Bag 16, Palapye, Botswana.
[4]Istituto Nazionale di Geofisica e Vulcanologia (INGV), Rome, Italy.
[5]Solar Physics Laboratory, NASA Goddard Space Flight Center, Greenbelt, 20771, MD, USA.
[6]The Catholic University of America, Washington, 20064, DC, USA.

*Corresponding author(s). E-mail(s): tesfayphysics@gmail.com;
Contributing authors: luca.spogli@ingv.it; ggabraha@gmail.com;

Abstract

We characterize the climatology of ionospheric scintillation and total electron content (TEC) over Ethiopia during the ascending phase of solar cycle 24. To the scope, seven years data (2008–2014) of TEC and amplitude scintillation (S4 index) recorded from two SCINDA (Scintillation Network and Decision Aid) GPS receivers installed at Addis Ababa (9.034°N, 38.67°E; geomagnetic 0.9°N, 110.5°E) and Bahir Dar (11.37°N, 37.10°E; geomagnetic 2.64°N, 108.94°E) were used. We arranged the data into long term hourly mean, diurnal mean, seasonal and yearly mean scales. The long term seasonal data grouped into D- season (January, February, November and December), E- season (March, April, September and October) and J-season (May, June, July and August). The long term hourly mean scintillation values in Addis Ababa and Bahir Dar have similar trend of occurrences during the Post-Sunset hours, i.e. 16:00 - 22:00UT (LT = UT+3 hour), with a peaking activity localized between 19:00 and 20:00 UT. In most observations of this study, the peak values of long term hourly mean (2008-2014)

of TEC was exhibited at 10:00 -14:00 UT, as a result of the ionospheric photo ionization process. We have classified the seven years data into seasonal mean during low solar activity (2008-2010) and high solar activity period (2011-2014); we observed that both TEC and scintillation occurrence during solar maxima was doubled to the values during solar minima period. This study revealed that climatological amplitude scintillations in East African equatorial region appeared at post sunset events and decrease around local midnight, with heighten activities in the months of March, April, October and September. Equinoctial asymmetry in scintillation occurs with higher occurrence during March and April than in September and October. Additionally, we investigate the relationship between geomagnetic storms and S4 events linked to Equatorial Plasma Bubbles (EPBs). Using the Izmiran Catalogue, we analyzed storm onset times and calculated the delay ($\boldsymbol{\Delta T}$) between storm commencement and local sunset. Our results show a significant increase in amplitude scintillation occurrence when $\boldsymbol{\Delta T}$ is less than 6 hours, highlighting the critical role of post-sunset geomagnetic activity in driving ionospheric irregularities. This finding provides new insights into scintillation variability and advances the understanding of low-latitude scintillation climatology.

Keywords: low latitude ionosphere, ionospheric scintillation, GNSS, equatorial plasma bubble

1 Introduction

Ionospheric plasma is generated by solar radiation and particle precipitation at high latitudes, which affect various geographic regions depending on the local time of day and the solar zenith angle. This results into an ionospheric density which varies from a maximum around the equatorial region to a minimum radiation at high latitudes. However, the sole photoionization is not enough to justify the morphology of the equatorial ionosphere. In fact, during the day a lower ionospheric density is measured at the magnetic equator, the so-called "ionospheric trough" (Appleton 1946) while a maximum is found off the magnetic equator, at around $\pm 15^{\circ}$ to $\pm 20^{\circ}$ magnetic latitudes, under solar maximum conditions (MacDougall 1969). These peaks are known as the EIA crests, formed by the fountain effect where plasma rises at the equator and diffuses poleward along magnetic field lines. This structure typically develops in late morning and persists until sunset (Appleton 1946). During the day time, the zonal electric field (E) flows eastward and it is mainly generated by a dynamo mechanism in the ionospheric E-region (Yamazaki and Maute 2017, and references therein), forming the so-called equatorial electrojet (EEJ). The interaction between the EEJ and Earth's magnetic fields leads the ionospheric plasma to be lifted upward vertically by the $\mathbf{E} \times \mathbf{B}$ drift, whose maximum effect is at the magnetic equator. While the plasma electrodynamics lifted up from the dip equator then, due to gravitational force and pressure gradient it diffuses downward along geomagnetic field lines of both hemispheres (Oryema et al. 2015; Balan et al. 2018; Abdu 2005). This plasma pattern formation is called the "plasma fountain" effect, which then develops higher electron

density on both sides, referred to as crests of EIA, while a small concentration of electron density has remained around zero degree magnetic latitude, referred to as trough of EIA. However, this equatorial structure of the crest and trough varies with latitudes of both hemispheres with the conditions of the day, season of the year, and solar activity (Chakraborty and Hajra 2009).

Near sunset at low latitudes, a pre-reversal enhancement (PRE) of the eastward electric field occurs, driving upward plasma drift. This is followed by an eastward field intensification immediately after sunset, before the field eventually reverses to westward (Rishbeth 1971; Fejer 1991) . The enhancement of eastward electric field prior to reversal of westward electric field is called "pre-reversal enhancement electric field (PRE)", which arises due to the development of F-region dynamo electric field under the local time of post sunset decay of the E layer conductivity (Fejer 1991; Heelis 2004; Woodman 1970). This PRE can blow up the F region plasma density profile from 100 to 200 km beyond its regular altitude. In the equatorial region the configuration of PRE can initiate the formation of Rayleigh-Taylor instability, which triggers the formation of ionospheric irregularities and consequently large electron density depletions formed along the magnetic lines called Equatorial Plasma Bubbles (EPBs) (Yokoyama 2017). The formation of EPBs and their development to small-scale ionospheric structures is a very complex phenomenon, that shows presents large variability both under quiet (day-to-day and small-scale variabilities) and disturbed (storm-time response) conditions (see, e.g., Balan et al. 2018; Abdu 2019; Li et al. 2021). The small-scale irregularities embedded in the EPBs poses serious threats to trans-ionospheric signals. Among these, those causing ionospheric scintillation are the most threatening for high-precision positioning services based on the use of signals emitted by Global Navigation Satellite Systems (GNSSs), spread of ionospheric echoes which threatens the for HF communication.

Specifically ionospheric scintillations are sudden and rapid fluctuations in the amplitude and phase of trans-ionospheric signals and are due to the diffraction of electromagnetic waves through small-scale structures in the ionospheric electron density encountered along the signal path (Wernik et al. 2003). Fading of the GNSS amplitude signals due to the irregularities embedded in the EPB can be greater than 25 dB, causing loss of lock of GNSS signals, decrease of the number of available GNSS satellites for positioning, and communication/navigation failures that can seriously jeopardize GNSS-based positioning (Cesaroni et al. 2015; Seo et al. 2009; Spogli et al. 2016).

Despite the general features of the GNSS scintillation occurrence are well consolidated in the literature, such as solar flux, seasonal, diurnal, temporal, and inter-annual variations, their modeling is still challenging and the storm-time behaviour and short-term and day-to-day variabilities represent an open field of research about magnetosphere-ionosphere-thermosphere-lower atmosphere coupling.

The precarious behavior of ionospheric irregularities in equatorial and low-latitude regions has been the subject of significant study, especially in the African sector. Tilahun and Asmare Tariku (2019) verified the ionospheric perturbation induced L-band scintillations using HF/VHF bands over Ethiopia in 2014. They observed that post sunset increases in hmF2(maximum height of the F2 layer), combined with

decreases in foF2(critical frequency of F2 layer) and significant TEC variations, seeding to the ionospheric irregularities and scintillation activities. Their findings revealed the intense scintillation activities occurred from 16:00 UT (19:00 LT) to 23:00 UT (02:00 LT), with peak Vertical Perturbation Index (PI) occurring at altitudes between 250–450 km, closely associated to hmF2. Furthermore, they investigated that, the VHF (Very High Frequency) bands experienced stronger scintillations and wider spectral noise compared to UHF (Ultra High Frequency), revealing frequency-dependent scintillation effects. These results underscore the utility of HF/VHF bands in verifying L-band scintillations and identifying ionospheric irregularities.

Expanding on this, Akala et al. (2017) investigated the climatology of scintillation at Addis Ababa between 2009 and 2013, focusing on strong scintillation events (S4 $\geq$ 0.5). Their results indicated that scintillation values enhanced during equinox months, while the lowest values was recorded in June and November. Our findings align with theirs in confirming that equinox months revealing the most significant scintillation occurrence. However, an important distinction lies in the methodology, that Akala et al. (2017) considered only strong scintillation events (S4 $\geq$ 0.5), whereas our study includes a lower threshold (S4 $\geq$ 0.1), capturing a broader range of scintillation activity. This difference likely explains why they reported almost no scintillation activity in June, whereas our analysis reveals that, although equinox months remain dominant, the June solstice indicates higher long-term S4 values compared to the December solstice at both Addis Ababa and Bahir Dar. Furthermore, while the study of Akala et al. (2017) used a subset of our data (2009-2013) and focused solely on Addis Ababa, our study extends the analysis to a longer period (2008-2014) and includes both Addis Ababa and Bahir Dar. This extensive dataset enables for a more comprehensive investigation of scintillation variability between the two stations and solar cycle phases, highlighting the differences between solar minimum (2008-2010) and solar maximum (2011-2014). Our results indicate that scintillation is significantly increases during periods of high solar activity, providing deeper insights into the influence of the solar cycle on ionospheric behavior.

Similarly, Seba and Gogie (2015) studied scintillation at Bahir Dar using data from August 2010 to July 2011. Their results showed that nighttime scintillation activity was lowest at the December solstice and highest during the equinox months, with slightly stronger scintillation levels during the June solstice compared to December. Our study confirms their observation that the December solstice exhibits weaker nighttime scintillation compared to the June solstice and supports the finding that equinox months experience the most intense scintillation activity. However, while their study was based on short-term data covering only one year, our research covers seven years (2008-2014) and includes data from both Addis Ababa and Bahir Dar. This wider dataset provides us to analyze long-term patterns, including the impact of the solar cycle on both scintillation and VTEC. Unlike Seba and Gogie (2015), who focused only on S4 variations, our study integrates VTEC data, showing that Bahir Dar indicates larger S4 variations while Addis Ababa experiences greater VTEC differences, particularly in the December solstice. Additionally, we provide a detailed comparison of solar minimum and solar maximum phases, illustrating the influence of solar activity on ionospheric variability.

Beyond these comparisons, our research introduces a new approach by investigating the relationship between geomagnetic storms and S4 events linked to Equatorial Plasma Bubbles (EPBs). Utilizing the Izmiran Catalogue, we analyzed storm onset times and calculated the delay (ΔT) between storm commencement and local sunset. Our findings reveal a significant increase in amplitude scintillation occurrence when ΔT is less than six hours, emphasizing the crucial role of post-sunset geomagnetic activity in driving ionospheric irregularities. This insight provides a deeper understanding of scintillation variability and advances knowledge in low-latitude scintillation climatology.

By incorporating a more extensive dataset across the two stations, accounting for both S4 and VTEC variations, differentiating between solar minimum and maximum phases, and exploring the influence of geomagnetic storms on EPBs(equatorial plasma bubbles), our study provides a more comprehensive understanding of ionospheric behavior over Ethiopia. Our findings reinforce key trends observed in previous studies while offering new insights into long-term variability and the effects of both the solar cycle and geomagnetic activity on ionospheric scintillation and VTEC.

Hence, our objective in this seven-year dataset investigation is to draw a climatological picture of the African equatorial ionospheric scintillation and TEC over Ethiopia, leveraging observations made in Addis Ababa (9.034°N, 38.67°E; geomagnetic 0.9°N, 110.5°E) and Bahir Dar (11.37°N, 37.10°E; geomagnetic 2.64°N, 108.94°E). This study contributes to the growing body of space weather research in Africa, as highlighted by Baki et al. (2023), who provide a comprehensive overview of the current status of space weather infrastructure and research across the continent. Our climatological result would have a significant role to design robust architecture for transequatorial GNSS-based avionics, navigations and other several higher frequency radio communications. In addition to that, following (Akala et al. 2010; Bilitza et al. 2004), we arranged the long data into daily, monthly, seasonally, and annually time sets. We believe that this study incorporating other African equatorial stations will then have an input to develop a regional-based scintillation and TEC model. Therefore, this study has been structured into sections of; Sect. 2 describes the data and methodology, Sects. 3–5 present the results and discussion, and Sect. 6 gives the conclusions.

2 Data and Methodologies

2.1 Data

Two data types namely, solar flux conditions described by solar flux (F10.7) and SCINDA-GPS data taken S4 and VTEC data were used. Employing dual-frequency GPS observations, it is possible to calculate the GPS-derived vTEC. In the equatorial F-region, post-sunset plasma density irregularities often develop through the uplift of bottom-side plasma via the Rayleigh-Taylor instability, creating field-aligned plasma depletions. These depletions appear as localized TEC reductions when integrated along satellite signal paths. The resulting electron density gradients simultaneously produce both amplitude (S_4) and phase (σ_ϕ) scintillations on trans-ionospheric signals from GPS and geostationary satellites (Abdu et al. 2009; Dashora and Pandey 2005).

Rayleigh Taylor Instability is considered as the physical mechanism of plasma bubbles at equatorial regions generated few hours after sunset and which are ionospheric TEC depletions. The GPS data recorded in the dual- frequency receivers have been utilized for this study, and the GPS- TEC data are estimated from pseudo range and carrier phase measurements on L1 and L2. The final TEC value is obtained after the removal of the satellite and receiver biases as follows (Ciraolo et al. 2006; Tariku 2015; Tornatore et al. 2021; Cesaroni et al. 2021):

$$\mathrm{TEC} = \mathrm{TEC}_R - (b_R + b_S) \tag{1}$$

where b_R and b_S are the receiver and satellite biases, respectively, and TEC_R is the relative TEC given as

$$\mathrm{TEC}_R = \mathrm{TEC}_\phi + \langle \mathrm{TEC}_P - \mathrm{TEC}_\phi \rangle_{\mathrm{arc}} \tag{2}$$

The differential pseudo-range (TEC_P) and differential carrier phase (TEC_ϕ) are obtained from

$$\mathrm{TEC}_P = \frac{1}{40.3}\left[\frac{f_1^2 f_2^2}{f_1^2 - f_2^2}\right](P_2 - P_1) \tag{3}$$

and

$$\mathrm{TEC}_\phi = \frac{1}{40.3}\left[\frac{f_1^2 f_2^2}{f_1^2 - f_2^2}\right](\phi_2 - \phi_1) \tag{4}$$

where $\langle\cdot\rangle_{\mathrm{arc}}$ is the average over a phase-connected arc. Vertical TEC (VTEC) is obtained from slant TEC as (Bagiya et al. 2009; Oluwadare et al. 2019)

$$\mathrm{VTEC} = \frac{\mathrm{TEC}_R - (b_R + b_S)}{S(\varepsilon)} \tag{5}$$

where $S(\varepsilon)$ is the single-layer mapping function of the ionosphere, defined as

$$S(\varepsilon) = \sec\left\{\sin^{-1}\left[\frac{R_e \cos\varepsilon}{R_e + h}\right]\right\} \tag{6}$$

Here ε is the elevation angle, R_e is the Earth's radius in kilometres and h is the height of the ionospheric shell. Using a trigonometric identity, Eq. (6) can be rewritten as

$$S(\varepsilon) = \left(1 - \left[\frac{R_e \cos\varepsilon}{R_e + h}\right]^2\right)^{-1/2} \tag{7}$$

This study used the amplitude scintillation index (S4), given by Briggs and Parkin (1963); Yeh and Liu (1982)

$$S_4 = \sqrt{\frac{\langle I^2\rangle - \langle I\rangle^2}{\langle I\rangle^2}} \tag{8}$$

where I is the signal intensity, computed by squaring the amplitude of the received signal, and $\langle\cdot\rangle$ denotes the ensemble average. The intensity of scintillation I^2 depends

on the radio wave frequency. The scintillation is mainly caused by plasma density irregularities with scale sizes below the first Fresnel scale (Li et al. 2021; Yeh and Liu 1982), defined as

$$D_f = \sqrt{2\lambda z} \tag{9}$$

where z is the height of the irregularity layer and λ is the radio wavelength. For the GPS L1 frequency (1575.42 MHz) and a vertical propagation geometry with $z =$ 400 km, the first Fresnel scale is about 390 m.

2.2 Solar Activity

Solar activity has an extensive impact on ionospheric plasma dynamics, and it mainly influences the plasma density distribution. Solar activities have significant roles in controlling the climatological variation of ionospheric irregularities and total electron content production. Thus, we used the two solar activity parameters, i.e. sunspot number (R) and solar flux (F10.7 cm). Solar flux is radio emission of the sun at the wavelength of 10.7 cm and 2800 MHz frequency.

Specifically, ionospheric seasonal ionization level variations is mainly due to solar zenith angle change, while its solar cycle variation is related to a change in solar EUV and X-ray radiation fluxes (Schunk and Nagy 2009; Kelley 2009). The VTEC and S4 variability is modulated by solar activity.

The variations in VTEC and S4 also occur due to the tilt and rotation of the Earth around the sun, and change in the intensity of radiation with geographical location. Table 1 shows the mean of SSN and solar flux (F10.7 cm) along time series covering the period from 2008 to 2014. The annual mean values of solar flux and sunspot number ranges 69 - 146 and 4.15 – 113.41 respectively. The maximum value of solar cycle 24 was reached in 2014. Similarly, a moderate enhancement of solar activity has been shown in 2011, 2012, and 2013 with a peak value of f10.7 reaching 253.3, in 2014.

2.3 Methodology

The essence of the climatological study is to assess long-time data to understand the general trend of the ionospheric dynamics of ionospheric irregularities (Povero et al. 2017), which may be important for different ionospheric scintillation models. Therefore, to investigate the climatology ionospheric scintillation it is important here to understand seasonal variations of amplitude scintillation, S4, and VTEC of seven years (2008-2014) data. Hence, we have classified each year into three seasons, i.e. E-season (March, April, September, and October), J-season (May, June, July, and August), and D-season (November, December, January, and February). While we grouped months into each season, the long-term diurnal hourly mean values for every four months have been also calculated. The S4 and VTEC, data sets are for seven years covering solar cycle 24. This solar cycle in turn has also been segmented into solar minima (2008-2010) and solar maxima (2011-2014) periods. All GNSS data were pre-processed with a 30° elevation mask prior to VTEC and S4 analysis, eliminating low angle signals susceptible to multipath distortion. VTEC values were first calculated using Eq. (5), accounting for receiver and satellite biases, then analyzed with an hourly centered moving average along with concurrent S4 indices. This consistent smoothing approach

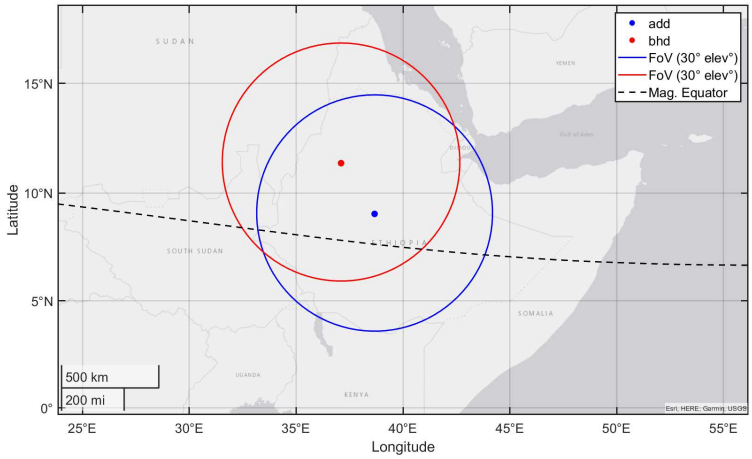

Fig. 1 SCINDA station locations in equatorial East Africa, with the geomagnetic field configuration. The broken curved line indicates the dip equator, and the fields of view (30° elevation) for Addis Ababa (blue) and Bahir Dar (red) are shown.

preserved diurnal patterns while reducing noise. The identical processing of both parameters maintained temporal coherence for comparative analysis of ionospheric irregularities.

Figure 1 illustrates the SCINDA network in equatorial East Africa, highlighting the geomagnetic field configuration. The stations in Addis Ababa (blue) and Bahir Dar (red) are located at different latitudes, allowing them to monitor how ionospheric irregularities change with the solar terminator and its impact on scintillation. The positions of the stations relative to the geomagnetic equator and the solar terminator are crucial, as they influence the ionospheric density and irregularities that develops the amplitude scintillation. The EIA, which peaks off dip equator, is most pronounced during the evening and night hours when the solar terminator is near the stations. This phenomenon can lead to increased scintillation during these periods, particularly when the solar terminator crosses through the equatorial region (Mersha et al. 2021; Wiens et al. 2006; Amabayo et al. 2014; Paznukhov et al. 2012). The field of view at 30 degrees from both Addis Ababa and Bahir Dar captures the area most affected by such ionospheric irregularities, providing insights into their geographic variability and evolution throughout the day as the terminator moves (Amabayo et al. 2014).

3 Results and Discussion

This section focuses on characterizing climatology of ionospheric amplitude scintillation and VTEC observed in two low latitudes SCINDA GPS receiver stations' data, collected during solar cycle 24. In this study we have used seven years of data, averaged into diurnal and seasonal variations. Here, the daytime, nighttime, seasonal and inter-annual characteristics of scintillation and VTEC have been discussed. In addition, our analysis of the climatological characteristics of scintillation and TEC during

solar cycle 24-phase has been classified into solar maxima and minima. Furthermore, this study investigates the relationship between amplitude scintillation (S4) and geomagnetic storms, with a specific focus on the post-sunset period, when ionospheric irregularities are most pronounced. Based on the local solar terminator, statistical relationships of S4 along with geomagnetic storm have been analyzed for each year.

Table 1 Yearly mean and maximum sunspot number (SSN) and solar flux F10.7 over the period of the GPS data (2008–2014)

	Sunspot number		F10.7 (sfu)	
Year	Mean	Max	Mean	Max
2008	4.16	60.0	68.98	88.2
2009	4.78	46.0	70.55	84.2
2010	24.87	69.0	79.97	93.1
2011	80.84	194.0	113.28	191.6
2012	84.54	174.0	120.03	183.7
2013	94.02	206.0	122.67	174.0
2014	113.41	220.0	145.98	253.3

3.1 Long-term diurnal variation of S4 and VTEC

Figure 2 shows the long-term (2008–2014) hourly mean VTEC and S4 for January to June. Figure 3 shows the same quantities for July to December at the two equatorial GPS stations.

At both Addis Ababa and Bahir Dar SCINDA-GPS receiver stations, the value of the hourly mean of VTEC gradually decreases during the early morning between 00:00–03:00 UT (LT = UT+ 3 hour) which agree with previous studies (Oyedokun et al. 2020; Tariku 2020). The long term hourly mean VTEC steadily increased after early morning attaining maximum values between noon and pre sun-set (9-15 UT),followed by decrease.

There is a slight variation from month to month. The minimum hourly long term S4 values are attained between 00:00–17:00 UT, steadily arising to maximum values around 19:00-21:00 UT, and followed by decrease to minimum at 24:00 UT. During which hours, the ionospheric density is largely dependent on the neutral winds, the recombination rate of electrons, and electric fields (Chapman 1954).

During some of the months (see Fig. 2), the hourly long-term VTEC mean at Bahir Dar is slightly higher than that at Addis Ababa, which may be due to the equatorial plasma fountain effect.

Moreover, there is a slight shift in the local time of occurrence of peak VTEC and S4 between the two stations. Bahir Dar leads Addis Ababa by about a fraction of an hour. Addis Ababa is located near the equator compared to Bahir Dar resulting in a slight enhancement of VTEC and S4 over Bahir Dar (nearest to equatorial plasma

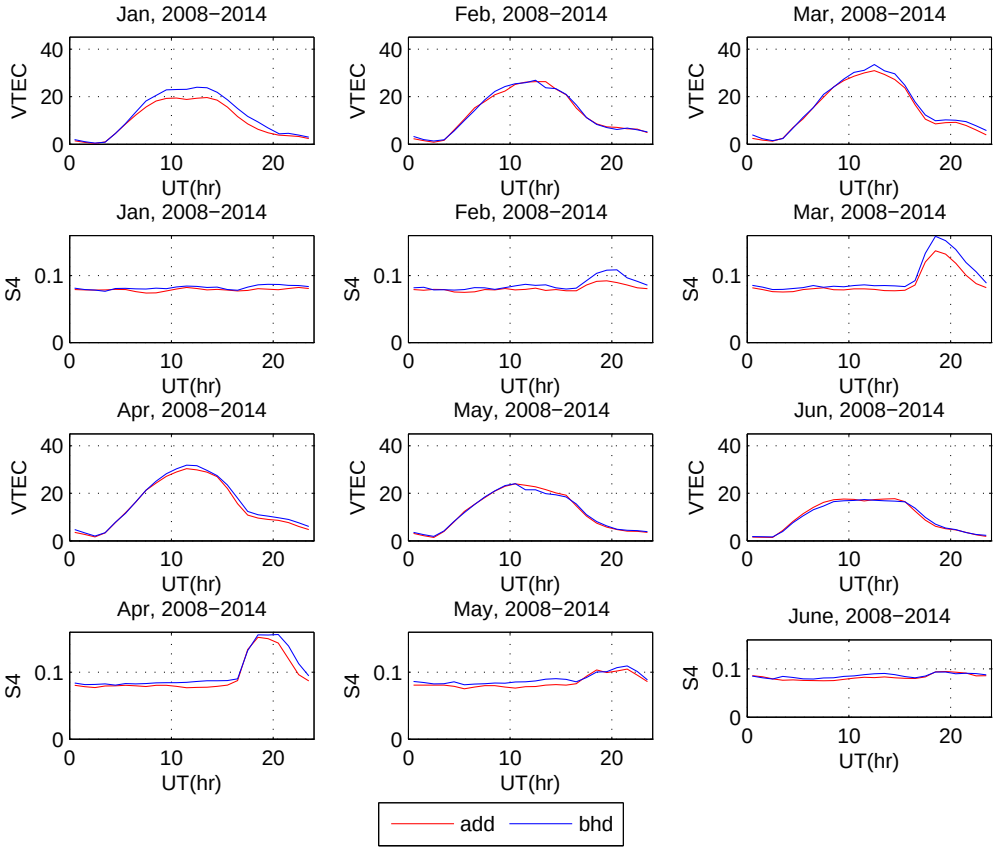

Fig. 2 Long-term mean (2008-2014) of hourly averaged VTEC and S4 for January to June at the Addis Ababa (red) and Bahir Dar (blue) GPS sites. The first and third rows show the hourly mean diurnal variation of VTEC, while the second and fourth rows show that of the S4 index. Data were smoothed using a centered hourly moving average before averaging across years.

crest relative to Addis Ababa) in contrast to Addis Ababa during January, February, March, and April. On the magnitude of VTEC over Addis Ababa is slightly greater the overhead than that of Bahir Dar during August, September, October, November, and December. Equinoxial asymmetry has been observed between March-April (maximum TEC and S4) and September-October (minimum TEC and S4) consistent with studies in East Africa (Abiriga et al. 2021; Olwendo et al. 2013). This scintillation equinoctial asymmetry could be attributed to the asymmetry of neutral winds in the thermosphere that drives the eastward electric fields (Olwendo et al. 2013). The climatological L-band scintillation study in Brazil (Cesaroni et al. 2015) has been concluded that even though the maximum values of TEC has observed during the fall season, the enhanced S4 driven by post sun-set TEC fluctuation is observed during spring than fall. However the presence of gradients alone is not sufficient to trigger scintillation. Instead, the large variability of the gradients themselves must have been responsible according to (Cesaroni et al. 2015) studies.

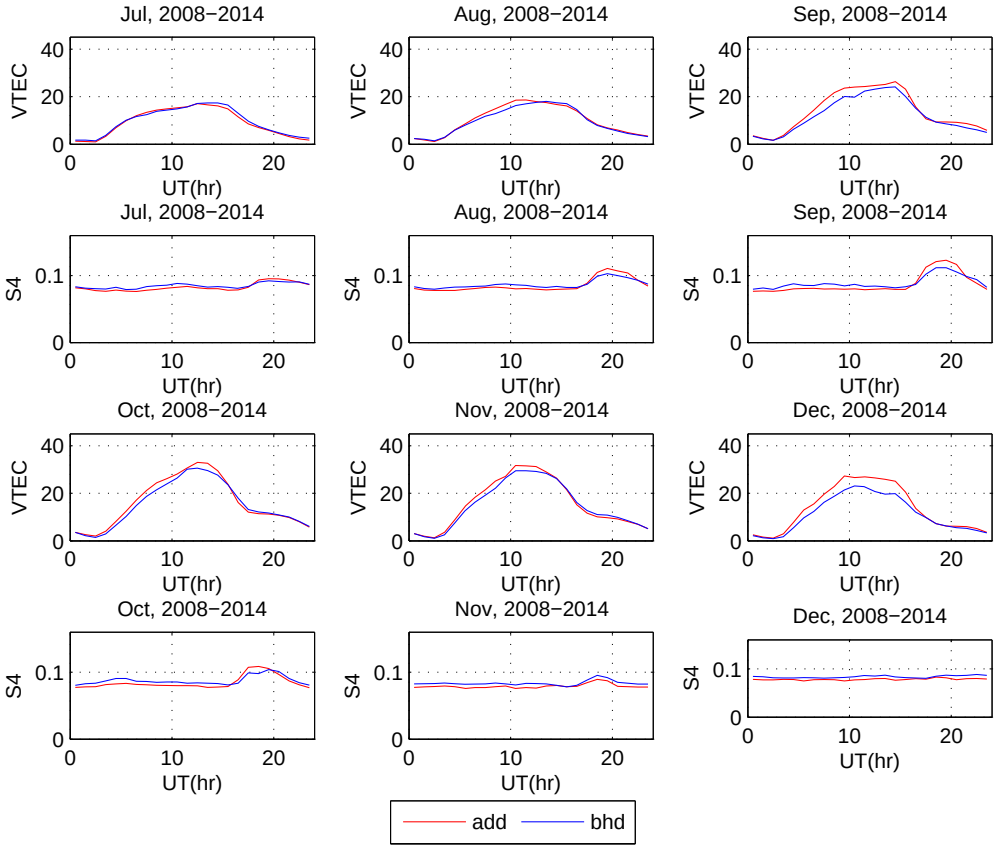

Fig. 3 Same as Fig. 2, but for July to December

The maximum VTEC and S4 occur during the equinox months and with fair moderate values observed during solstice months. The minimum TEC is attained during June and July and the least amplitude scintillation appeared in January, which is in agreement with multiple studies (Akala et al. 2014; Olwendo et al. 2013). Even though the predominant enhancement of TEC was attained in the daytime, a small enhancement of TEC has been exhibited during nighttime during equinox months which drops again after a few hours of midnight. The nighttime enhancement has been reported other studies (Adewale et al. 2012; Mukherjee et al. 2010; Oron et al. 2013). Previous studies (Galav et al. 2010; Tariku 2015) reported that the night-time enhancement can be associated with PRE, which is attributed to the variation of plasma drift in the F-region. Intense scintillations were observed during March and April months, followed by September and October with moderate values, as noted from the long-term mean S4 in Figs. 2 and 3.

3.2 Long term mean diurnal variabilities of VTEC and S4 during the two phases of solar cycle 24 in D, E, and J seasons

According to Lloyd's seasonal classification (Eyelade et al. 2017), based on the solar radiation the year is classified into three seasons. Such classifications includes D-Season or December Solstice (November, December, January, and February), E-Season or Equinox months (March, April, September, and October), and J-Season or June Solstice (May, June, July, and August) seasons (Amaechi et al. 2020, references therein).

Figures 4 and 5 show VTEC and amplitude scintillation that were observed by GPS receivers at Addis Ababa and Bahir Dar, during solar cycle phase 24 (2008 -2014) split into seasons of solar minimum (2008-2010) and maximum (2011-2014). The first rows in both Figs. 4 and 5 show TEC and the second rows show amplitude scintillation (S4) for Solar Maximum and Solar minimum at Addis Ababa and Bahir Dar stations respectively. The figures depict VTEC and S4 in Addis Ababa and Bahir Dar during low solar activity (green for TEC and black color for S4) and maximum phase solar activity (blue for TEC and red for S4).

The climatology that, enhanced amplitude scintillation occurs more often during E-season (see middle column, bottom panels in Figs. 4 and 5) followed by J-season. Moreover, the peak values of VTEC were attained during the maximum solar activity period during E-season followed by D-season, in agreement with the study (Eyelade et al. 2017). The minimum amplitude scintillation was observed during D-season of the solar maximum period.

The S4 scintillation onset exhibits solar cycle dependence, with E-season occurring at ∼15:10 UT (18:10 LT) during solar maxima and shifting to ∼16:00 UT (19:00 LT) during minima. For J-season, onset remains at ∼16:00 UT (19:00 LT) during maxima. While these results show general agreement with the Brazilian climatology of Sousasantos et al. (2018) (showing ∼20:00 LT onset in November/December), the observed ∼1-hour difference likely reflects local time/longitudinal variations in scintillation characteristics.

Table 2 Relative difference of the seasonal peak S4 and peak VTEC between solar maximum (2011–2014) and solar minimum (2008–2010), computed as $(X_{\max} - X_{\min})/X_{\max} \times 100$, at Addis Ababa (Add) and Bahir Dar (Bhd)

	S4 difference (%)		VTEC difference (%)	
Season	Add	Bhd	Add	Bhd
D	8.49	12.93	60.09	53.57
E	37.54	40.11	54.51	47.28
J	18.41	22.71	48.55	46.00

The seasonal variability of VTEC and S4 values during low and high solar activity phases at both Addis Ababa and Bahir Dar stations reveals significant differences (Table 2). At Addis Ababa, the peak VTEC during solar maximum exceeds the values observed during solar minimum by 60.09% in D-season, 54.51% in the E-season, and 48.55% in J-season. Similarly, the peak S4 index increases by 8.49%, 37.54%, and 18.41% in D, E, and J-seasons, respectively. Conversely, Bahir Dar exhibits slightly lower VTEC enhancements, with increases of 53.57%, 47.28%, and 46.00% in D, E, and J-seasons, respectively. In contrast, the S4 index at Bahir Dar shows relatively higher differences, reaching 12.93% in D-season, 40.11% in E-season, and 22.71% in J-season. These results indicate that both stations experience a strong response to solar activity, particularly during the equinox (E-season), where the VTEC and S4 differences are most pronounced. However, while Bahir Dar exhibits slightly larger S4 variations in all seasons, Addis Ababa shows greater VTEC differences, especially in the D-season. The observed TEC and S_4 differences between Bahir Dar (11.37°N, dip 2.64°N) and Addis Ababa (9.034°N, dip 0.9°N) reveal three interhemispheric effects: (1) Bahir Dar's proximity to the northern Equatorial Ionization Anomaly (EIA) crest enhances plasma density irregularities compared to Addis Ababa's near-equatorial position; (2) seasonal thermospheric wind asymmetries preferentially amplify plasma transport into Bahir Dar's hemisphere during solstices; (3) Bahir Dar's slightly western (1.6° east) shifts irregularity onset by approximately 10 minutes earlier relative to Addis Ababa. Figures 4, 5 demonstrate these mechanisms through consistently stronger TEC and S_4 enhancements at Bahir Dar, particularly during equinoxes when the fountain effect peaks. This enhancement may be associated with the equatorial plasma fountain effect that is attributable to the asymmetry effect of inter-hemispherical meridional winds and electric field distributions (Huang and Cheng 1996; Khadka et al. 2018).

During the E-season, amplitude scintillation enhancement occurs around 16:00 UT (peaking near 19:00 UT), while during the J-season, it occurs at 17:00 UT (peaking near 20:00 UT). This pattern aligns with studies of ionospheric irregularities in Africa (e.g., Amaechi et al. 2020) and climatological observations over Brazil (e.g., Muella et al. 2017; de Oliveira Moraes et al. 2018; Correia et al. 2018). This time difference between seasons may be attributed to the delayed reversal of the eastward electric field during the summer season in association with PRE (Abdu 2005).

3.3 Long-term mean diurnal variations of VTEC and S4 in D, E, and J seasons

Figure 6 depicts the variations of both parameters observed during D, E, and J-seasons at two low latitude sectors over Ethiopia. The enhanced VTEC and S4 are observed during E-season over Addis Ababa (Add) and Bahir Dar (Bhd), consistent with previous studies (Akala et al. 2011, 2014; Olwendo et al. 2013; Amaechi et al. 2020). D-season VTEC is the next maximum TEC due to the segregation of neutral winds and gases from the summer to the winter hemisphere, resulting in an enormous production of total electron content within the winter hemisphere caused by the increment of O/N_2 ratio.

Furthermore, the moderate scintillation that was attained during J-season was higher than the scintillation during D-season which is consistent with Seba and Gogie

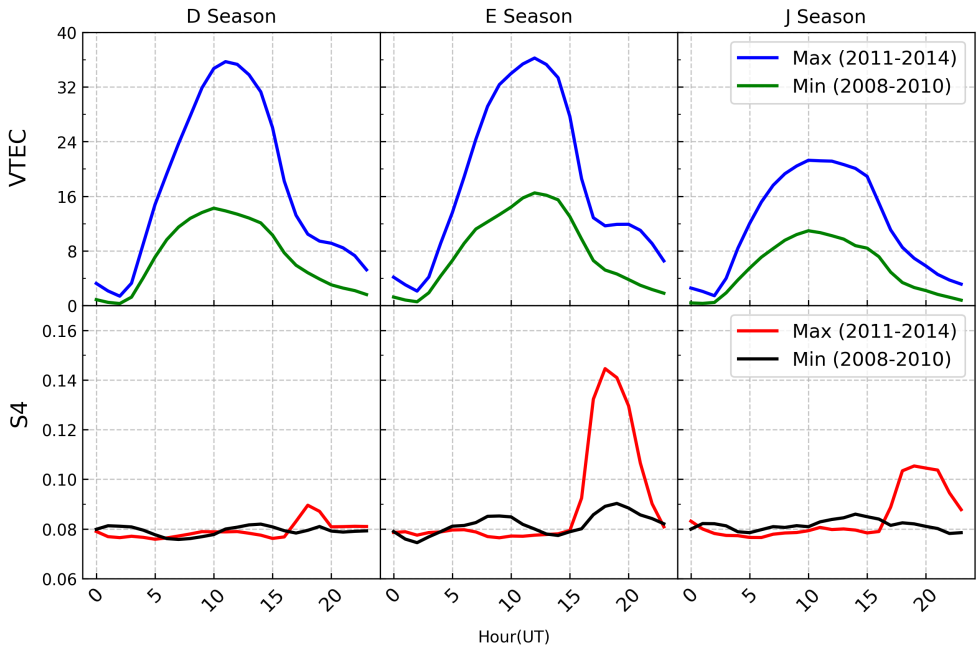

Fig. 4 The seasonal mean of VTEC (top row) and S4 (bottom row) during low solar activity (2008-2010) represented by green color for VTEC and black for S4 and the high solar activity period (2011-2014) represented by blue for VTEC and red color for S4 at Addis Ababa station.

(2015). This is because scintillation can intensify during rainy seasons, particularly at equatorial latitudes, where it may also coincide with signal attenuation (Karasawa et al. 1988). The maximum enhanced mean VTEC was around 30 TECU at 13:00 UT in Addis Ababa and Bahir Dar, and the minimum VTEC was less than 5 TECU at around 3:00 UT. The slightly higher VTEC and S4 values observed at Bahir Dar compared to Addis Ababa may be attributed to its proximity to the equatorial ionization anomaly (EIA) crest region, where TEC characteristically peaks. This enhanced scintillation could arise from stronger plasma density gradients near the EIA crest, combined with potential local wave activity or thermospheric dynamics that preferentially affect Bahir Dar's longitudinal sector.

During all phases of solar activity, heating asymmetry has occurred due to transportation of neutral constituents from summer (J-season) to winter (D-season) hemisphere, consequently, the recombination rate in the winter hemisphere falls, resulting in peak VTEC (Torr and Torr 1973). Furthermore, during northern summer (J-season) the direction of the meridional component of the neutral wind can cause decaying of EIA crest value as it blows in the opposite direction of plasma diffusion originating from the magnetic equator (Bhuyan and Borah 2007; Wu et al. 2004). Meanwhile, winter anomaly i.e. greater peak VTEC appeared during winter (D-season) than its conjugate summer (J-season). However, greater S4 has been recorded in the summer.

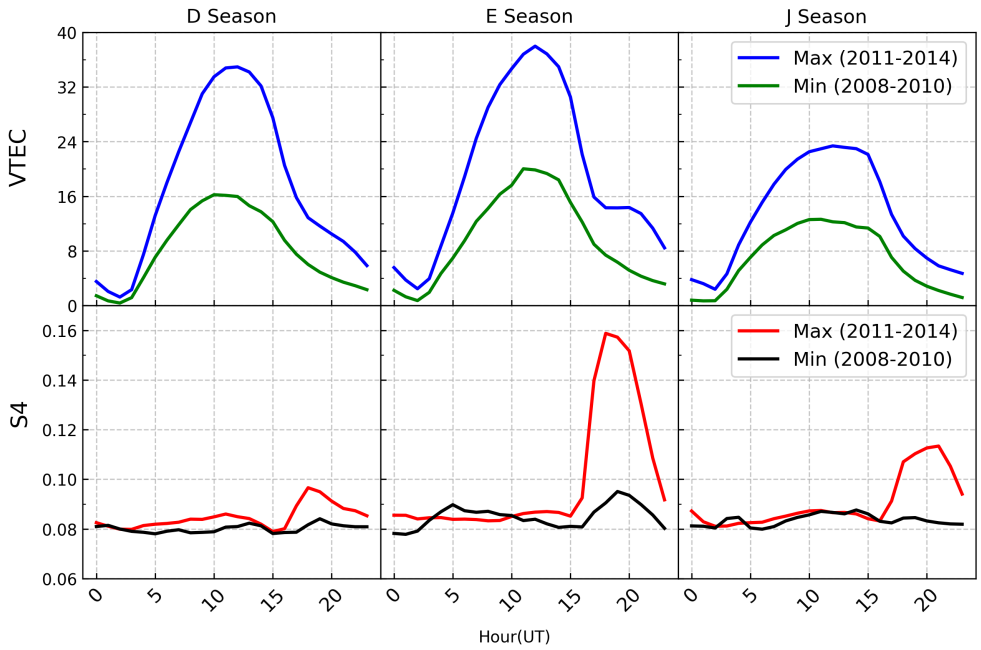

Fig. 5 Same as Fig. 4, but for the Bahir Dar SCINDA GPS station

Similarly, greater S4 during J-season may be caused by electric field fluctuations. This could be due to the direction of the inter-hemispheric wind from summer to winter, and atmospheric gravity waves including large-scale waves (Amaechi et al. 2020; Tesema et al. 2017; Tsunoda et al. 2010). In addition, studies have shown that the presence of strong post-midnight irregularities in the June solstice is due to the Rayleigh Taylor instability.

This climatological study reveals the presence of weak ionospheric scintillations (small S4 values) during the summer solstitial months (J-season). Although these fluctuations are near the noise level, their local time distribution strongly associates them with equatorial plasma bubble (EPB) activity. This interpretation is supported by recent findings from Cesaroni et al. (2025), who observed scintillation events over Malindi (Kenya) closely tied to the pre-reversal enhancement (PRE) of the zonal electric field. During the summer solstice, scintillations coincide with a PRE that peaks before sunset, despite having a lower magnitude compared to equinoctial conditions. The weaker PRE acts on a denser background plasma, still generating a sufficient bottom-side density gradient to destabilize the ionosphere and trigger EPBs. In comparison, the winter solstice features a stronger PRE, but its occurrence after the solar terminator passage at ionospheric heights inhibits EPB development. This seasonal asymmetry explains the subdued yet discernible scintillation activity observed during the J-season, distinguishing it from both equinoctial and winter solstitial periods.

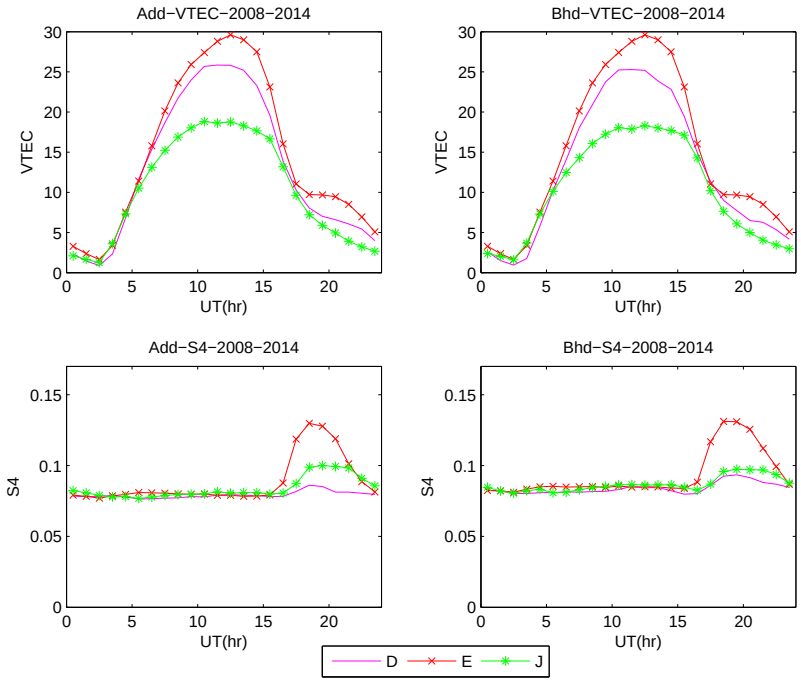

Fig. 6 The seasonal mean of VTEC (top row) and S4 (bottom row) during solar cycle 24 at Addis Ababa and Bahir Dar SCINDA GPS stations. The purple, red, and green colors represent the D, E, and J-seasons respectively.

3.4 Inter-annual variations of seasonal mean VTEC and S4

Figures 7 and 8 illustrate the interannual variability of VTEC and S4, both of which exhibit a monotonic increase following the pattern of solar activity. Figure 7 shows that the frequency of S4 observations is higher in Bahir Dar than in Addis Ababa, but both locations exhibit a similar trend, with solar activity governing their variations. Figure 8 presents the hourly mean variations of VTEC and S4 as a function of the year, revealing distinct hourly fluctuations in VTEC across all seasons from 2008 to 2014. During the D, E, and J seasons, both VTEC and S4 values increase monotonically from the solar minimum (2008) to the solar maximum (2014). Meanwhile, amplitude scintillation over Addis Ababa and Bahir Dar stations commonly appeared after late sunset and before sunrise. These parameters that depend on latitude, longitude, season, and solar activity may well influence the characteristics of climatological ionospheric scintillation. Hence, Figs. 7 and 8 exhibited both long-term mean values of TEC, and scintillation was highly determined by solar activities. When the mean solar activity of F10.7 and sunspot number attains 122.67 and 94 respectively in 2013, the profound value of TEC was observed during D-season than the other equinox season. This observation of enhanced TEC during December solstice in 2013 was reported by Akala et al. (2015a) and the reason may be due to TEC transportation from middle latitude to lower latitude and the Earth is closest to the Sun (perihelion, about 147

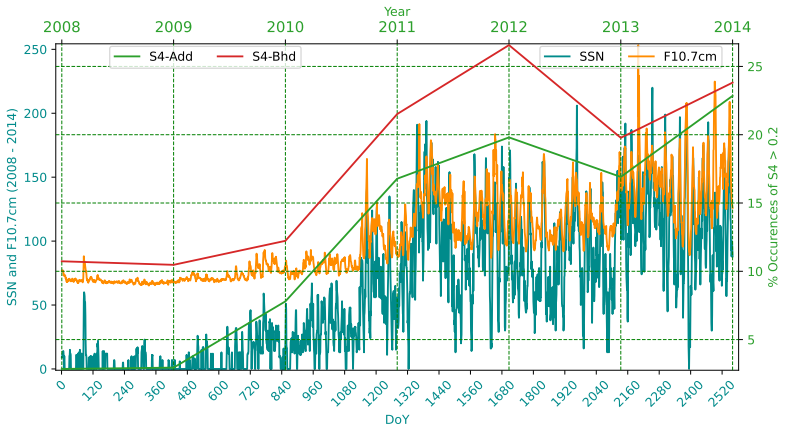

Fig. 7 Yearly percentage occurrence of S4 > 0.2 at Addis Ababa (green) and Bahir Dar (red) during Solar Cycle 24 (2008–2014), with daily sunspot number (SSN, teal) and F10.7 (orange). The bottom axis counts days from 1 January 2008

million km) during the D-season. Meanwhile, both climatological amplitude scintillation and TEC values around the magnetic equator increase along with the maximum phase of solar activity; consequently enhanced ionization density at the F-region and plasma irregularities have occurred at the background of enhanced ionization density (Macho et al. 2021). Whereas climatological ionospheric scintillation is low during low solar activity, this is a good attribute as amplitude scintillation around the magnetic equator has a strong connection with the level of ionization density. The trend of yearly S4 and TEC values are a function of the solar activity for each year, consequently, both activities are low in 2008 and reach peak values during the active solar phenomenon (see Fig. 7).

4 Diurnal Variation of S4 During Solar Maximum and Minimum Periods

Figures 9–12 present heatmaps depicting the daily variation of ionospheric amplitude scintillation (S4) during solar maximum (2011–2014) and solar minimum (2008–2010) at the Add and Bhd stations. The color scale on the right represents S4 intensity, with darker shades indicating lower values and lighter shades denoting higher values. Additionally, vertical blue lines mark the approximate times of sunrise (left line) and sunset (right line), considering the ionospheric pierce point (IPP) at 120 km altitude. These contour maps provide insights into the temporal distribution of S4 and its dependence on solar activity cycles.

A notable insight observed from the contour maps is the predominance of S4 scintillation during the post-sunset and nighttime, which is strongly associated with equatorial plasma bubbles (EPBs). These EPBs are driven by the Rayleigh-Taylor instability, which plays a significant role in the production of S4 scintillation. This finding aligns with recent studies in the same region, such as that by Cesaroni et al. (2025), who also reported enhanced post-sunset scintillation activity associated with EPBs

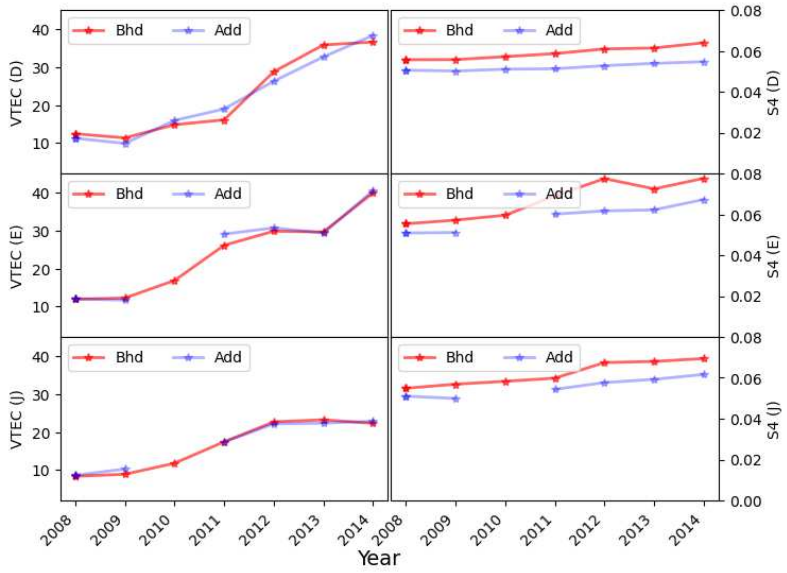

Fig. 8 The interannual and seasonal variability of VTEC and S4 index over Bahir Dar and Addis Ababa. The x-axis represents the year, while the left and right y-axes correspond to VTEC and S4 index, respectively. The S4 index includes all values starting from its minimum, providing a complete representation of scintillation activity. Red and blue lines indicate Bahir Dar and Addis Ababa, respectively.

and emphasized the significant influence of PRE in shaping ionospheric irregularities in the equatorial region.

The peak of occurrences is predominantly observed between 18:00 and 00:00 UT, which is consistent with the anticipated ionospheric irregularities that manifest subsequent to sunset. During the peak of solar activity (2011-2014), there exists a markedly pronounced and extensive manifestation of S4, particularly surrounding the equinox months of March-April and September-October. In comparison, during the solar minimum (2008-2010), the occurrences of S4 are considerably diminished, featuring fewer high-intensity regions(Amabayo et al. 2017). The observable presence of substantial white spaces within the contour maps during the solar minimum period indicates intervals characterized by data gaps, attributable to extensive power disruptions.

Hence this study, long-term diurnal S4 variability from SCINDA stations in Addis Ababa and Bahir Dar were analyzed, revealing significant post-sunset scintillation activity with a significant equinoctial pattern. Due to the distinct geographic positioning and geometric considerations, the average time of sunset terminator in Addis Ababa precedes that of Bahir Dar by a fractional number of hours. The observed S4 and vTEC values were slightly higher in Bahir Dar than in Addis Ababa, consistent with the longitudinal variability of equatorial ionospheric irregularities (Yizengaw and Groves 2018) and attributed to the equatorial ionization anomaly (EIA) effect, as observed over Brazil by Macho et al. (2021). This difference can be attributed to Bahir Dar's later local sunset time as noted in the above, which, combined with its closer

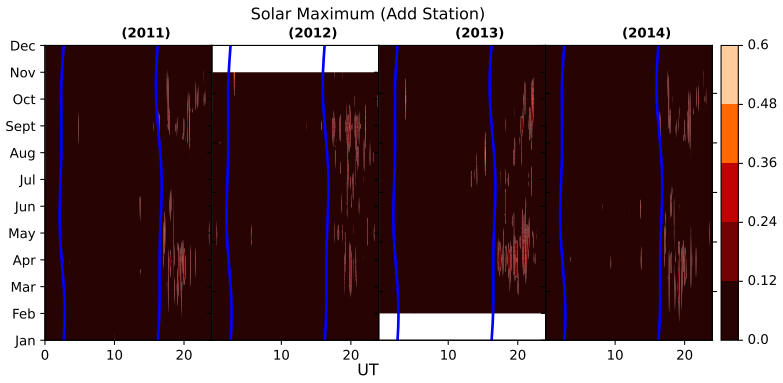

Fig. 9 Distribution of S4 during solar maximum (2011–2014) of Solar Cycle 24 over Addis Ababa (Add)

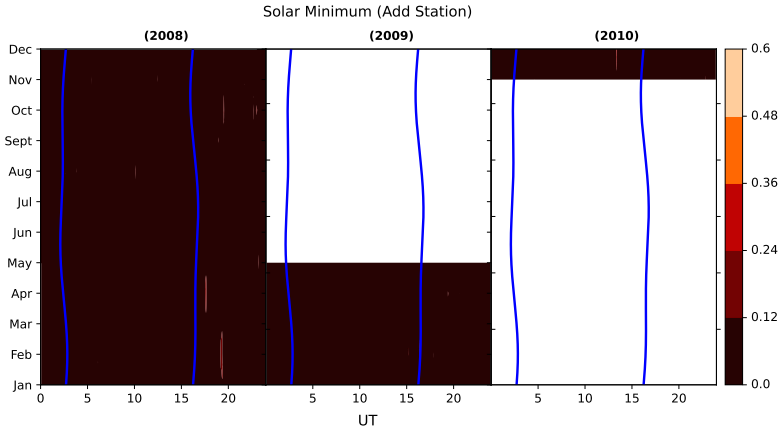

Fig. 10 Same as Fig. 9, but for solar minimum (2008–2010)

alignment to the magnetic equator, enhances the PRE-driven instability and favors stronger EPB formation compared to Addis Ababa.

5 Equatorial Plasma Bubbles and S4

The phenomenon of photoionization demonstrates an extended duration at elevated altitudes within the ionosphere, particularly in the F-layer, as opposed to the diminished durations observed in the lower D and E-layers; consequently, the transport mechanisms exert a significant influence on the F-layer, facilitating its sustenance throughout the nighttime. Therefore, it is imperative to consider the implications of the sunset terminator on the amplitude scintillation, with this study focusing exclusively on the F-layer at altitudes exceeding 120 km. In order to conduct a comparative analysis of the effects of the sunset terminator on S4 at both Addis Ababa and Bahir Dar stations, we utilized their respective geographic coordinates.

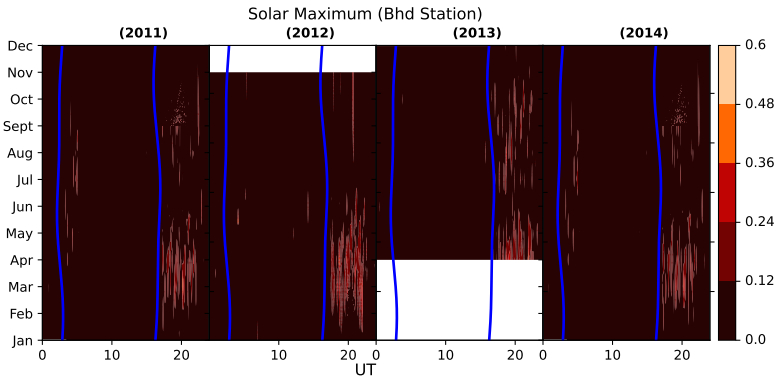

Fig. 11 Distribution of S4 during solar maximum (2011–2014) of Solar Cycle 24 over Bahir Dar (Bhd)

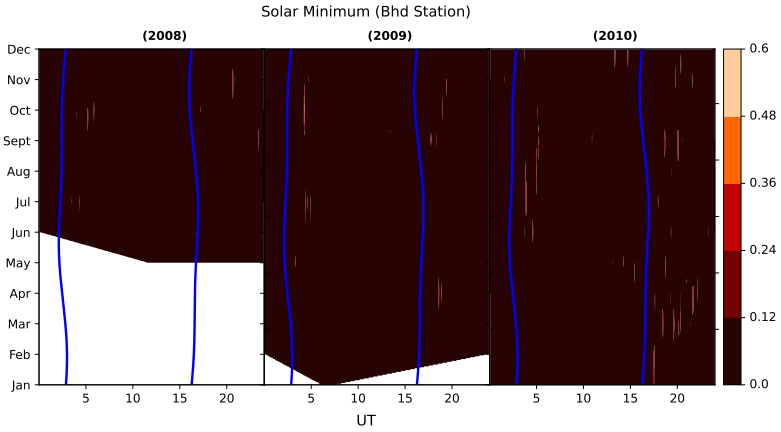

Fig. 12 Same as Fig. 11, but for solar minimum (2008–2010)

The amplitude scintillation usually produced due to the development of EPBs, which is affected by the dynamics between magnetic declination, and the solar terminator and seasonal patterns that correlate with solar activity cycles(Abdu et al. 1981; Yizengaw and Groves 2018). These seasonal variations further highlight the complex interplay between solar activity, solar terminator, and magnetic declination dynamics (Abdu et al. 1992).

In this section, the solar terminator is analyzed in the context of equatorial plasma bubble (EPB) formation, with a focus on the pre-reversal enhancement (PRE) of the zonal electric field, which is a primary driver of EPB seeding. The PRE is strongly associated with the dynamics of the equatorial electrojet (EEJ) (Akala et al. 2015b), and thus, the sunset times were evaluated relative to the magnetic equator rather than the geographic locations of the SCINDA receivers. This approach aligns with the methodology employed in various recent studies, that emphasized the importance of considering the magnetic equator for better investigation of longitudinal variabilities

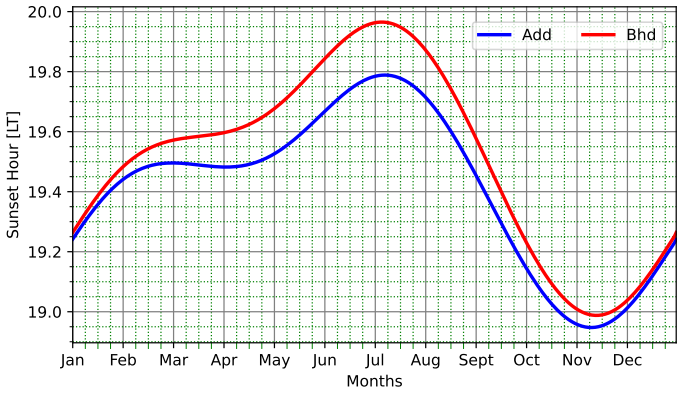

Fig. 13 Sunset time as a function of day of year for Addis Ababa (blue) and Bahir Dar (red), computed at the ionospheric pierce point (IPP) altitude of 350 km.

(Cesaroni et al. 2025; Pica et al. 2025). Furthermore, the influence of geomagnetic activity on ionospheric variabilities, as highlighted by Spogli et al. (2024), underscores the need for a magnetic equator to consider the relationship between solar terminator dynamics and EPB generation. By adopting this approach, this study ensures a more robust interpretation of the observed scintillation patterns and their correlation with post-sunset ionospheric irregularities.

Figure 13 distinctly illustrates the local sunset times for Addis Ababa (depicted in blue) and Bahir Dar (depicted in red) at an azimuth angle of 105°. The angle between the magnetic declination and the solar terminator plays a vital role to produce an equatorial plasma bubbles (EPBs) by altering the dynamics of the ionosphere. EPBs are substantially generated when the angle between the magnetic declination and solar terminator tends to zero (i.e., during the equinoxes), as this activity enhances the formation and growth of EPBs(Mersha et al. 2021).

The PRE, being the main seeding process ruling out the EPB occurrence, is strictly influenced by the solar terminator and the magnetic declination(Huba 2016; Picanço et al. 2024). Particularly, the duration of sunset in the conjugate E region affects by magnetic declination, which in turn influences the development of electric fields in the F region. Various research outputs reveal that the differences in declination angles causes to change the vertical ionization drift velocities, which significantly affect the development of spread F and the formation of EPBs (Abdu et al. 1981).

Furthermore, the solar terminator, which designated as the boundary between day and night, produces medium-scale traveling wave packets that vary the ionospheric irregularities. Many observational studies showing that these wave packets appear instantly after the solar terminator passes, suggesting that have a direct connection between the position of the terminator and the production of EPBs (Afraimovich et al. 2010). The position of the terminator and timing, with respect to the magnetic declination, thus play a vital role in altering ionospheric disturbances and EPB formation.

Figures 14 and 15 show the relationship between geomagnetic storms and the frequency of S4 events, which may be associated to the emergence of Equatorial

Plasma Bubbles (EPBs). The Izmiran Catalogue was employed to analyze storm commencement times. By identifying the storm onset time (t_{storm}) from the OMNI catalog, we computed the time delay ΔT between local sunset and storm onset as $\Delta T = t_{\text{storm}} - t_{\text{sunset}}$, where t_{sunset} is the local sunset time (converted to UT) and t_{storm} the storm sudden commencement (SSC) time. This ΔT parameter was then used to analyze the relationship between storm arrival time and post-sunset scintillation occurrence at Bahir Dar and Addis Ababa. The frequency of scintillation events (S4 $>$ 0.1) was then analyzed as a function of ΔT for various seasons (winter, summer, and equinox) across multiple years. The analysis builds on previous findings that storms occurring near post-sunset hours can enhance EPB formation due to the intensified pre-reversal enhancement (PRE) of the ionospheric electric field (Paznukhov et al. 2012). This study aims to further elucidate the relationship between storm dynamics and EPB occurrence, providing insights into how variations in solar activity influence ionospheric behavior during different seasonal conditions.

At Addis Ababa, the results revealed a strong seasonal dependence of scintillation activity. Equinox seasons exhibited the highest frequencies of S4 $>$ 0.1, particularly for storms occurring within 5 hours after local sunset (ΔT between 0 and 5 hours). During 2011, 2012 and 2014, for instance, scintillation occurrence reached up to 50 in equinox months, indicating enhanced EPB seeding during these periods (Seba and Gogie 2015). In contrast, summer and winter seasons showed markedly lower scintillation occurrence, with almost less activity in winter. This can be attributed to the reduced post-sunset ionospheric gradients and weaker storm-driven PRE effects, which are less favorable for EPB formation (George Erick 2017).

Similarly, Bahir Dar station exhibited higher scintillation occurrence during equinox seasons, with the number of events reaching up to 65 in some cases, such as in 2014. This further supports that storm onsets near sunset during equinox periods significantly amplify EPB activity. Summer and winter seasons, however, exhibited reduced scintillation activity, in agreement with the observations at Addis Ababa. Though, Bahir Dar and Addis Ababa are located within the same equatorial region, the scintillation onset at Bahir Dar was typically delayed by $\sim$30 minutes compared to Addis Ababa. Moreover, the S4 index values tended to be slightly higher at Bahir Dar during equinoctial months. These differences may be attributed to small-scale variations in the equatorial ionization anomaly and local magnetic declination, influencing the generation and propagation of irregularities. Similar localized effects were discussed by Seba and Nigussie (2016).

The comparative analysis conducted in this study reveals consistent trends of increased EPB activity during equinox seasons for ΔT values of less than 6 hours, supporting the hypothesis that shorter delays between storm onset and sunset maximize the probability of EPB formation by facilitating the coupling of storm-induced electric fields to the ionosphere during periods of strong post-sunset ionospheric. The significantly lower scintillation occurrence observed during summer and winter further highlight the importance of seasonal variation in modulating storm effects on EPBs (Abiriga et al. 2020).

This study identified a strong correlation between post-sunset S4 enhancements, geomagnetic storms and seasonal dependencies, highlighting the role of storm-time

electric fields in modulating scintillation activity. These findings align with the longitudinal and seasonal dependencies of EPBs and scintillation discussed by Yizengaw and Groves (2018).

The observed time delay (ΔT) between storm onset and local sunset highlights the importance of storm-time electric fields in modulating equatorial plasma bubble (EPB) formation. During geomagnetic storms, the ionospheric response is driven by two primary mechanisms: prompt-penetrating electric fields (PPEFs) and disturbance dynamo electric fields (DDEFs). PPEFs, which occur almost immediately after storm onset, are caused by the direct penetration of high-latitude electric fields into the equatorial ionosphere, often enhancing the pre-reversal enhancement (PRE) and promoting EPB growth. In contrast, DDEFs develop more gradually, typically hours after the storm onset, and are associated with thermospheric wind perturbations that alter the ionospheric electric field configuration, often suppressing EPB formation. The interplay between these mechanisms can explain the observed variability in post-sunset scintillation activity during storms, as reported in studies such as (Yamazaki and Maute 2017; Li et al. 2021; Spogli et al. 2021). For example, Spogli et al. (2021) demonstrated how PPEFs and DDEFs influenced ionospheric irregularities over Brazil during the August 2018 geomagnetic storm, providing a framework for understanding similar effects in other equatorial regions, including East Africa. These findings underscore the need to consider both PPEFs and DDEFs when analyzing storm-time EPB dynamics and their impact on scintillation.

The observed seasonal scintillation patterns demonstrate strong alignment with established equatorial climatology, showing peak S4 activity during equinoxes (70-80% occurrence in March-April; 50-60% in September-October) as documented by Akala et al. (2015a) and Abiriga et al. (2021), consistent with solar terminator-geomagnetic field alignment. The expected December solstice minimum (3.3-5.2%) was evident, though June solstice activity exceeded the November occurrence rates (40%) reported by Akala et al. (2015a). This discrepancy may reflect longitudinal variations in geomagnetic geometry (Yizengaw and Groves 2018), thermospheric wind patterns, or differing observational periods (2008-2014 versus 2011). The results show consistency with NORISK project findings (Cesaroni et al. 2025) and regional studies (Olwendo et al. 2013), while highlighting the importance of continuous long-term monitoring for resolving temporal variations in scintillation climatology.

6 Conclusions

This study examined ionospheric scintillation and TEC variability over Ethiopia from 2008 to 2014, encompassing solar cycle 24. Results show that S4 enhancements are strongly linked to pre-reversal enhancement (PRE)-driven plasma uplift, especially around midnight at both Addis Ababa and Bahir Dar. VTEC peaks occurred at 13:00–14:00 UT, while S4 peaked at 19:00–20:00 UT, highlighting distinct diurnal patterns. Seasonally, both VTEC and S4 were highest during the equinoctial (E) season, moderate in June solstice (J), and weakest in the December solstice (D). These variations align with solar radiation levels and ionospheric dynamics, such as daytime plasma uplift and nighttime diffusion. Notably, PRE-induced VTEC enhancements

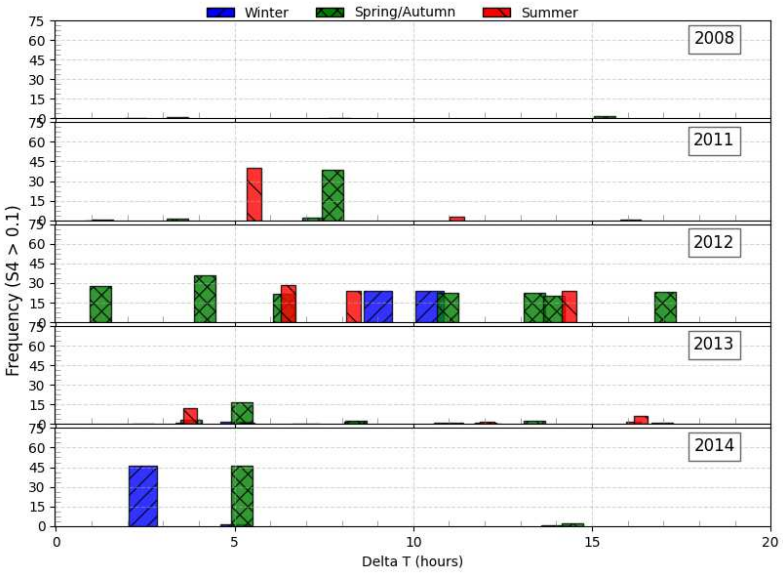

Fig. 14 Statistical analysis of EPBs at the Add station, after sunset and during a geomagnetic storm, based on the IZMIRAN geomagnetic storm catalogue. Blue, green and red represent winter (D-season), equinox (E-season) and summer (J-season), respectively

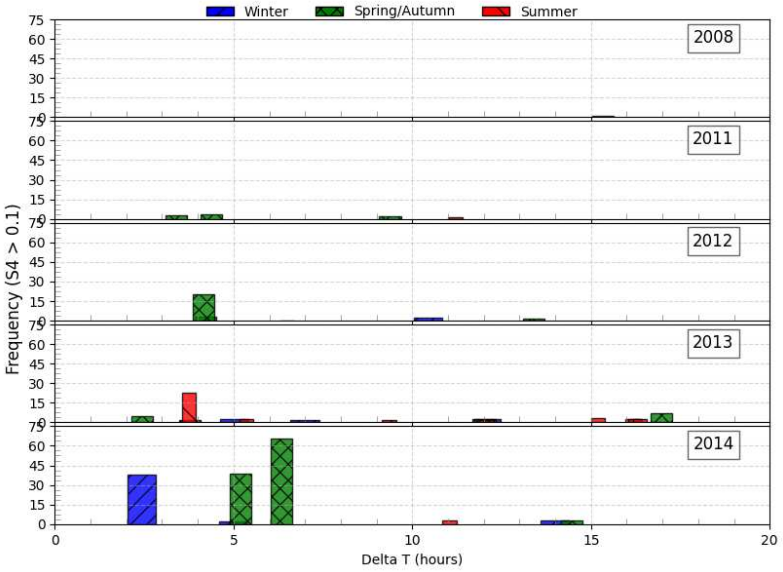

Fig. 15 Same as Fig. 14, but for the Bahir Dar (Bhd) station

were observed at midnight during the E-season, often coinciding with strong scintillation. Yearly comparisons revealed that both VTEC and S4 nearly doubled from the solar minimum (2008–2010) to the maximum (2011–2014). Monthly analysis indicated that March and April had the highest S4 values, while January and June recorded the lowest. Scintillation strength was also found to correlate with sunspot number, reinforcing the influence of solar activity.

The study identified enhanced post-sunset scintillation, peaking around 22:00 LT near the magnetic equator. Equinoctial asymmetry and the winter anomaly were also evident, potentially driven by changes in the $[O]/[N_2]$ ratio. These features underscore the complex interplay between neutral composition, solar inputs, and ionospheric irregularities. Importantly, we found a significant increase in scintillation occurrence when geomagnetic storms began within 6 hours after local sunset. This timing-sensitive relationship suggests that both local-time dynamics and geomagnetic activity play a critical role in modulating scintillation. This aspect, less explored in previous studies, offers new insight into EPB formation and irregularity development.

This work contributes to the understanding of a comprehensive climatological assessment of amplitude scintillation and TEC over East Africa, advancing our understanding of their temporal, seasonal, and solar cycle variations. It also introduces a novel framework for evaluating the combined effects of post-sunset periods and geomagnetic storms. Future studies are encouraged to extend this analysis across different longitudes and space weather conditions to develop a more global understanding of scintillation behavior and its practical implications for communication and navigation systems.

Acknowledgements. We would like to express our gratitude to the Space Science and Geospatial Institute (SSGI), Mekelle University, UNIVAP, NASA-GSFC, for providing access to their research facilities. We also extend our thanks to Addis Ababa and Bahir Dar Universities for supplying the seven-year SCINDA GPS TEC data used in this study. Additionally, we acknowledge the National Aeronautics and Space Administration (NASA) for making available the sunspot number and F10.7 cm flux data, which were accessed through https://omniweb.gsfc.nasa.gov/form/dx1.html. Finally, we appreciate the geomagnetic storm data provided by the Izmiran Space Weather Catalog, accessible at https://www.izmiran.ru/services/iweather/storm/.

Declarations

- **Funding:** TODO – state funding sources, or "The authors received no specific funding for this work."
- **Conflict of Interest:** On behalf of all authors, the corresponding author states that there is no conflict of interest.
- **Ethics approval and consent to participate:** Not applicable.
- **Consent for publication:** Not applicable.
- **Data availability:** The SCINDA GPS TEC and S4 data were provided by Addis Ababa University and Bahir Dar University and are available from the corresponding author on reasonable request. Sunspot number and F10.7 data are available

from NASA OMNIWeb (https://omniweb.gsfc.nasa.gov/form/dx1.html). Geomagnetic storm onset times are available from the IZMIRAN Space Weather Catalogue (https://www.izmiran.ru/services/iweather/storm/).

- **Code availability:** TODO – available from the corresponding author on reasonable request, or give a repository link.
- **Author contributions:** Tesfay Yemane Tesfu: Conceptualization, Methodology, Formal analysis, Data curation, Visualization, Writing the original draft. Luca Spogli: Conceptualization (the investigation of geomagnetic storm timing and post-sunset S4 occurrence using the storm onset-to-sunset delay, ΔT), Methodology, providing sample plots, review and editing. Gebregiorgis Abraha Fikade: Supervision, review and editing. Gizaw Mengistu Tsidu: Resources (provision of the SCINDA data), Conceptualization (long-term analysis), advising, reviewing and editing. Nat Gopalswamy: review and editing (solar cycle activity), guiding geomagnetic storm data sources. Seiji Yashiro: review and editing (solar cycle activity). All authors read and approved the final manuscript.

References

Abdu, M.A.: Equatorial ionosphere–thermosphere system: Electrodynamics and irregularities. Advances in Space Research **35**(5), 771–787 (2005) https://doi.org/10.1016/j.asr.2005.03.150

Abdu, M.A.: Day-to-day and short-term variabilities in the equatorial plasma bubble/spread f irregularity seeding and development. Progress in Earth and Planetary Science **6**(1) (2019) https://doi.org/10.1186/s40645-019-0258-1

Abdu, M.A., Bittencourt, J.A., Batista, I.S.: Magnetic declination control of the equatorial f region dynamo electric field development and spread f. Journal of Geophysical Research: Space Physics **86**(A13), 11443–11446 (1981) https://doi.org/10.1029/ja086ia13p11443

Abdu, M.A., Batista, I.S., Sobral, J.H.A.: A new aspect of magnetic declination control of equatorial spread f and f region dynamo. Journal of Geophysical Research: Space Physics **97**(A10), 14897–14904 (1992) https://doi.org/10.1029/92ja00826

Abdu, M.A., Alam Kherani, E., Batista, I.S., De Paula, E.R., Fritts, D.C., Sobral, J.H.A.: Gravity wave initiation of equatorial spread F/plasma bubble irregularities based on observational data from the SpreadFEx campaign. Annales Geophysicae **27**(7), 2607–2622 (2009) https://doi.org/10.5194/angeo-27-2607-2009

Abiriga, F., Amabayo, E.B., Jurua, E., Cilliers, P.J.: Statistical characterization of equatorial plasma bubbles over east africa. Journal of Atmospheric and Solar-Terrestrial Physics **200**, 105197 (2020) https://doi.org/10.1016/j.jastp.2020.105197

Abiriga, F., Amabayo, E.B., Jurua, E., Cilliers, P.J.: Investigation of the impact of Ionospheric Scintillation on GNSS Performance over East Africa. Advances in Space

Research **68**(7), 2876–2889 (2021) https://doi.org/10.1016/j.asr.2021.05.012

Adewale, A.O., Oyeyemi, E.O., Cilliers, P.J., McKinnell, L.A., Adeloye, A.B.: Low solar activity variability and IRI 2007 predictability of equatorial Africa GPS TEC. Advances in Space Research **49**(2), 316–326 (2012) https://doi.org/10.1016/j.asr.2011.09.032

Afraimovich, E.L., Edemsky, I.K., Voeykov, S.V., Yasukevich, Y.V., Zhivetiev, I.V.: Mhd nature of ionospheric wave packets generated by the solar terminator. Geomagnetism and Aeronomy **50**(1), 79–95 (2010) https://doi.org/10.1134/s001679321001010x

Akala, A.O., Oyeyemi, E.O., Somoye, E.O., Adeloye, A.B., Adewale, A.O.: Variability of foF2 in the African equatorial ionosphere. Advances in Space Research **45**(11), 1311–1314 (2010) https://doi.org/10.1016/j.asr.2010.01.003

Akala, A.O., Doherty, P.H., Valladares, C.E., Carrano, C.S., Sheehan, R.: Statistics of GPS scintillations over South America at three levels of solar activity. Radio Science **46**(5) (2011) https://doi.org/10.1029/2011RS004678

Akala, A.O., Amaeshi, L.L.N., Doherty, P.H., Groves, K.M., Carrano, C.S., Bridgwood, C.T., Seemala, G.K., Somoye, E.O.: Characterization of GNSS scintillations over Lagos, Nigeria during the minimum and ascending phases (2009-2011) of solar cycle 24. Advances in Space Research **53**(1), 37–47 (2014) https://doi.org/10.1016/j.asr.2013.09.034

Akala, A.O., Amaeshi, L.L.N., Somoye, E.O., Idolor, R.O., Okoro, E., Doherty, P.H., Groves, K.M., Carrano, C.S., Bridgwood, C.T., Baki, P., D'ujanga, F.M., Seemala, G.K.: Climatology of GPS amplitude scintillations over equatorial Africa during the minimum and ascending phases of solar cycle 24. Astrophysics and Space Science **357**(1) (2015) https://doi.org/10.1007/s10509-015-2292-9

Akala, A.O., Amaeshi, L.L.N., Somoye, E.O., Idolor, R.O., Okoro, E., Doherty, P.H., Groves, K.M., Carrano, C.S., Bridgwood, C.T., Baki, P., D'ujanga, F.M., Seemala, G.K.: Climatology of GPS amplitude scintillations over equatorial Africa during the minimum and ascending phases of solar cycle 24. Astrophysics and Space Science **357**(1) (2015) https://doi.org/10.1007/s10509-015-2292-9

Akala, A.O., Ejalonibu, A.H., Doherty, P.H., Radicella, S.M., Groves, K.M., Carrano, C.S., Bridgwood, C.T., Stoneback, R.A.: Characterization of GNSS amplitude scintillations over Addis Ababa during 2009–2013. Advances in Space Research **59**(8), 1969–1983 (2017) https://doi.org/10.1016/j.asr.2017.01.044

Amabayo, E.B., Edward, J., Cilliers, P.J., Habarulema, J.B.: Climatology of ionospheric scintillations and tec trend over the ugandan region. Advances in Space Research **53**(5), 734–743 (2014) https://doi.org/10.1016/j.asr.2013.12.015

Amabayo, E.B., Jurua, E., Cilliers, P.J.: Assessment of scintillation proxy maps for a scintillation study during geomagnetically quiet and disturbed conditions over uganda. Journal of Atmospheric and Solar-Terrestrial Physics **154**, 47–54 (2017) https://doi.org/10.1016/j.jastp.2016.12.009

Amaechi, P.O., Oyeyemi, E.O., Akala, A.O., Falayi, E.O., Kaab, M., Benkhaldoun, Z., Mazaudier, C.A.: Quiet Time Ionopheric Irregularities Over the African Equatorial Ionization Anomaly Region. Radio Science **55**(8) (2020) https://doi.org/10.1029/2020RS007077

Appleton, E.V.: Two anomalies in the ionosphere. Nature **157**(3995), 691 (1946) https://doi.org/10.1038/157691a0

Bagiya, M.S., Joshi, H.P., Iyer, K.N., Aggarwal, M., Ravindran, S., Pathan, B.M.: TEC variations during low solar activity period (2005-2007) near the equatorial ionospheric anomaly crest region in India. Annales Geophysicae **27**(3), 1047–1057 (2009) https://doi.org/10.5194/angeo-27-1047-2009

Baki, P., Rabiu, B., Amory-Mazaudier, C., Fleury, R., Cilliers, P.J., Adechinan, J., Emran, A., Bounhir, A., Cesaroni, C., Dinga, J.B., Doherty, P., Gaye, I., Ghalila, H., Grodji, F., Habarulema, J.-B., Kahindo, B., Mahrous, A., Messanga, H., Mungufeni, P., Nava, B., Nigussie, M., Olwendo, J., Sibanda, P., Loua, R.T., Uwamahoro, J., Zaourar, N., Zerbo, J.-L.: The status of space weather infrastructure and research in africa. Atmosphere **14**(12), 1791 (2023) https://doi.org/10.3390/atmos14121791

Balan, N., Liu, L., Le, H.: A brief review of equatorial ionization anomaly and ionospheric irregularities. Earth and Planetary Physics **2**(4), 1–19 (2018) https://doi.org/10.26464/epp2018025

Bhuyan, P.K., Borah, R.R.: TEC derived from GPS network in India and comparison with the IRI. Advances in Space Research **39**(5), 830–840 (2007) https://doi.org/10.1016/j.asr.2006.12.042

Bilitza, D., Obrou, O.K., Adeniyi, J.O., Oladipo, O.: Variability of f o F2 in the equatorial ionosphere. Advances in Space Research **34**(9), 1901–1906 (2004) https://doi.org/10.1016/j.asr.2004.08.004

Briggs, B.H., Parkin, I.A.: On the variation of radio star and satellite scintillations with zenith angle. Journal of Atmospheric and Terrestrial Physics **25**(6), 339–366 (1963) https://doi.org/10.1016/0021-9169(63)90150-8

Cesaroni, C., Spogli, L., Alfonsi, L., De Franceschi, G., Ciraolo, L., Galera Monico, J.F., Scotto, C., Romano, V., Aquino, M., Bougard, B.: L-band scintillations and calibrated total electron content gradients over Brazil during the last solar maximum. Journal of Space Weather and Space Climate **5** (2015) https://doi.org/10.1051/swsc/2015038

824 Cesaroni, C., Spogli, L., De Franceschi, G.: Ionoring: Real-time monitoring of the total
825 electron content over italy. Remote Sensing **13**(16), 3290 (2021) https://doi.org/10.
826 3390/rs13163290

827 Cesaroni, C., Pezzopane, M., Zuccheretti, E., Pica, E., Spogli, L., Okoh, D., Pignalberi,
828 A., Olwendo, J., Alfonsi, L., Marcocci, C., Romano, V., Imam, R., De Franceschi,
829 G., Nava, B., Habarulema, J.B., Santilli, G., Di Cecco, A., Munzer, J.: Establishing
830 the first ionospheric observatory in kenya: Early results from the norisk project.
831 Advances in Space Research (2025) https://doi.org/10.1016/j.asr.2025.01.051

832 Chakraborty, S.K., Hajra, R.: Electrojet control of ambient ionization near the crest
833 of the equatorial anomaly in the Indian zone. Annales Geophysicae **27**(1), 93–105
834 (2009) https://doi.org/10.5194/angeo-27-93-2009

835 Chapman, S.: Winds in the ionosphere. Physics Today **7**(7), 8–12 (1954) https://doi.
836 org/10.1063/1.3061716

837 Ciraolo, L., Azpilicueta, F., Brunini, C., Meza, A., Radicella, S.M.: Calibration errors
838 on experimental slant total electron content (tec) determined with gps. Journal of
839 Geodesy **81**(2), 111–120 (2006) https://doi.org/10.1007/s00190-006-0093-1

840 Correia, E., Muella, M.T.A.H., Alfonsi, L., Prol, F.S., Camargo, P.O.: GPS scintilla-
841 tions and total electron content climatology in the southern American sector. In:
842 Accuracy of GNSS Methods. IntechOpen, London (2018). https://doi.org/10.5772/
843 intechopen.79218

844 Dashora, N., Pandey, R.: Observations in equatorial anomaly region of total elec-
845 tron content enhancements and depletions. Annales Geophysicae **23**(7), 2449–2456
846 (2005) https://doi.org/10.5194/angeo-23-2449-2005

847 de Oliveira Moraes, A., Muella, M.T.A.H., Paula, E.R., Oliveira, C.B.A., Terra, W.P.,
848 Perrella, W.J., Meibach-Rosa, P.R.P.: Statistical evaluation of GLONASS amplitude
849 scintillation over low latitudes in the Brazilian territory. Advances in Space Research
850 **61**(7), 1776–1789 (2018) https://doi.org/10.1016/j.asr.2017.09.032

851 Eyelade, V.A., Adewale, A.O., Akala, A.O., Bolaji, O.S., Rabiu, A.B.: Studying the
852 variability in the diurnal and seasonal variations in GPS total electron content
853 over Nigeria. Annales Geophysicae **35**(3), 701–710 (2017) https://doi.org/10.5194/
854 angeo-35-701-2017

855 Fejer, B.G.: Low latitude electrodynamic plasma drifts : a review. Journal of Atmo-
856 spheric and Terrestrial Physics **53**(8), 677–693 (1991) https://doi.org/10.1016/
857 0021-9169(91)90121-M

858 Galav, P., Dashora, N., Sharma, S., Pandey, R.: Characterization of low latitude
859 GPS-TEC during very low solar activity phase. Journal of Atmospheric and Solar-
860 Terrestrial Physics **72**(17), 1309–1317 (2010) https://doi.org/10.1016/j.jastp.2010.

09.017

George Erick, O.: Quiet time correlation between geomagnetic field variations and the dynamics of the east african equatorial ionosphere. International Journal of Astrophysics and Space Science **5**(1), 6 (2017) https://doi.org/10.11648/j.ijass.20170501.12

Heelis, R.A.: Electrodynamics in the low and middle latitude ionosphere: A tutorial. Journal of Atmospheric and Solar-Terrestrial Physics **66**(10), 825–838 (2004) https://doi.org/10.1016/j.jastp.2004.01.034

Huang, Y.-N., Cheng, K.: Solar cycle variations of the equatorial ionospheric anomaly in total electron content in the asian region. Journal of Geophysical Research: Space Physics **101**(A11), 24513–24520 (1996)

Huba, J.D.: Effect of Magnetic Declination on Equatorial Spread F Bubble Development. Wiley (2016). https://doi.org/10.1002/9781118929216.ch20 . http://dx.doi.org/10.1002/9781118929216.ch20

Karasawa, Y., Yamada, M., Yasukawa, K.: Tropospheric scintillation in the 14/11-GHz bands on earth-space paths with low elevation angles. IEEE Transactions on Antennas and Propagation **36**(4), 563–569 (1988) https://doi.org/10.1109/8.1146

Kelley, M.C.: The Earth's Ionosphere: Plasma Physics and Electrodynamics, 2nd edn. Academic Press, Burlington, MA (2009)

Khadka, S.M., Valladares, C.E., Sheehan, R., Gerrard, A.J.: Effects of Electric Field and Neutral Wind on the Asymmetry of Equatorial Ionization Anomaly. Radio Science **53**(5), 683–697 (2018) https://doi.org/10.1029/2017RS006428

Li, G., Ning, B., Otsuka, Y., Abdu, M.A., Abadi, P., Liu, Z., Spogli, L., Wan, W.: Challenges to equatorial plasma bubble and ionospheric scintillation short-term forecasting and future aspects in East and Southeast Asia. Surveys in Geophysics **42**(1), 201–238 (2021) https://doi.org/10.1007/s10712-020-09613-5

MacDougall, J.W.: The equatorial ionospheric anomaly and the equatorial electrojet. Radio Science **4**(9), 805–810 (1969) https://doi.org/10.1029/rs004i009p00805

Macho, E.P., Correia, E., Spogli, L., Muella, M.T.d.A.H.: Climatology of ionospheric amplitude scintillation on gnss signals at south american sector during solar cycle 24 (2021) https://doi.org/10.21203/rs.3.rs-411913/v1

Mersha, M.W., Lewi, E., Jakowski, N., Wilken, V., Berdermann, J., Kriegel, M.: On the relationship between low latitude scintillation onset and sunset terminator over africa. Remote Sensing **13**(11), 2087 (2021) https://doi.org/10.3390/rs13112087

Muella, M.T.A.H., Duarte-Silva, M.H., Moraes, A.O., Paula, E.R., Rezende, L.F.C.,

Alfonsi, L., Affonso, B.J.: Climatology and modeling of ionospheric scintillations and irregularity zonal drifts at the equatorial anomaly crest region. Annales Geophysicae **35**, 1201–1218 (2017) https://doi.org/10.5194/angeo-35-1201-2017

Mukherjee, S., Sarkar, S., Purohit, P.K., Gwal, A.K.: Seasonal variation of total electron content at crest of equatorial anomaly station during low solar activity conditions. Advances in Space Research **46**(3), 291–295 (2010) https://doi.org/10.1016/j.asr.2010.03.024

Oluwadare, T.S., Nguyen Thai, C., Akala, A.O.O., Heise, S., Alizadeh, M., Schuh, H.: Characterization of GPS-TEC over African equatorial ionization anomaly (EIA) region during 2009–2016. Advances in Space Research **63**(1), 282–301 (2019) https://doi.org/10.1016/j.asr.2018.08.044

Olwendo, O.J., Baluku, T., Baki, P., Cilliers, P.J., Mito, C., Doherty, P.: Low latitude ionospheric scintillation and zonal irregularity drifts observed with GPS-SCINDA system and closely spaced VHF receivers in Kenya. Advances in Space Research **51**(9), 1715–1726 (2013) https://doi.org/10.1016/j.asr.2012.12.017

Oron, S., D'ujanga, F.M., Ssenyonga, T.J.: Ionospheric tec variations during the ascending solar activity phase at an equatorial station, Uganda. Indian Journal of Radio and Space Physics **42**(1), 7–17 (2013)

Oryema, B., Jurua, E., D'Ujanga, F.M., Ssebiyonga, N.: Investigation of TEC variations over the magnetic equatorial and equatorial anomaly regions of the African sector. Advances in Space Research **56**(9), 1939–1950 (2015) https://doi.org/10.1016/j.asr.2015.05.037

Oyedokun, O.J., Akala, A.O., Oyeyemi, E.O.: Characterization of African Equatorial Ionization Anomaly During the Maximum Phase of Solar Cycle 24. Journal of Geophysical Research: Space Physics **125**(9), 0–2 (2020) https://doi.org/10.1029/2019JA027066

Paznukhov, V.V., Carrano, C.S., Doherty, P.H., Groves, K.M., Caton, R.G., Valladares, C.E., Seemala, G.K., Bridgwood, C.T., Adeniyi, J., Amaeshi, L.L.N., Damtie, B., D'Ujanga Mutonyi, F., Ndeda, J.O.H., Baki, P., Obrou, O.K., Okere, B., Tsidu, G.M.: Equatorial plasma bubbles and l-band scintillations in africa during solar minimum. Annales Geophysicae **30**(4), 675–682 (2012) https://doi.org/10.5194/angeo-30-675-2012

Pica, E., Spogli, L., Cesaroni, C., Alfonsi, L., Haralambous, H., Vallianatos, F., De Franceschi, G., Romano, V., Marcocci, C.: Assessing the ionospheric scintillations occurrence on l-band in the southern mediterranean sector. Advances in Space Research **75**(1), 837–855 (2025) https://doi.org/10.1016/j.asr.2024.10.032

Picanço, G.A.S., Denardini, C.M., Nogueira, P.A.B., Fagundes, P.R., Meza, A.M., Mendoza, L.P.O., Pádua, M.B., Natali, M.P., Resende, L.C.A., Vital, L.F.R.: On

the role of physical processes in controlling equatorial plasma bubble morphology. Journal of Geophysical Research: Space Physics **129**(9) (2024) https://doi.org/10.1029/2024ja032756

Povero, G., Alfonsi, L., Spogli, L., Di Mauro, D., Cesaroni, C., Dovis, F., Romero, R., Abadi, P., Le Huy, M., La The, V., Floury, N.: Ionosphere monitoring in south east Asia in the ERICA study. Navigation, Journal of the Institute of Navigation **64**(2), 273–287 (2017) https://doi.org/10.1002/navi.194

Rishbeth, H.: Polarization fields produced by winds in the equatorial F-region. Planetary and Space Science **19**(3), 357–369 (1971) https://doi.org/10.1016/0032-0633(71)90098-5

Schunk, R.W., Nagy, A.F.: Ionospheres: Physics, Plasma Physics, and Chemistry, 2nd edn. Cambridge University Press, Cambridge (2009). https://doi.org/10.1017/CBO9780511635342

Seba, E.B., Gogie, T.K.: Characterization of ionospheric scintillation at a geomagnetic equatorial region station. Advances in Space Research **56**(10), 2057–2063 (2015) https://doi.org/10.1016/j.asr.2015.07.035

Seba, E.B., Nigussie, M.: Investigating the effect of geomagnetic storm and equatorial electrojet on equatorial ionospheric irregularity over east african sector. Advances in Space Research **58**(9), 1708–1719 (2016) https://doi.org/10.1016/j.asr.2016.06.037

Seo, J., Walter, T., Chiou, T.Y., Enge, P.: Characteristics of deep GPS signal fading due to ionospheric scintillation for aviation receiver design. Radio Science **44**(4), 1–10 (2009) https://doi.org/10.1029/2008RS004077

Sousasantos, J., De Oliveira Moraes, A., Sobral, J.H.A., Muella, M.T.A.H., Paula, E.R.D., Paolini, R.S.: Climatology of the scintillation onset over southern Brazil. Annales Geophysicae **36**(2), 565–576 (2018) https://doi.org/10.5194/angeo-36-565-2018

Spogli, L., Cesaroni, C., Di Mauro, D., Pezzopane, M., Alfonsi, L., Musicò, E., Povero, G., Pini, M., Dovis, F., Romero, R., Linty, N., Abadi, P., Nuraeni, F., Husin, A., Le Huy, M., Lan, T.T., La, T.V., Pillat, V.G., Floury, N.: Formation of ionospheric irregularities over southeast asia during the 2015 st. patrick's day storm. Journal of Geophysical Research: Space Physics **121**(12) (2016) https://doi.org/10.1002/2016ja023222

Spogli, L., Sabbagh, D., Regi, M., Cesaroni, C., Perrone, L., Alfonsi, L., Di Mauro, D., Lepidi, S., Campuzano, S.A., Marchetti, D., De Santis, A., Malagnini, A., Scotto, C., Cianchini, G., Shen, X.H., Piscini, A., Ippolito, A.: Ionospheric response over brazil to the august 2018 geomagnetic storm as probed by cses-01 and swarm satellites and by local ground-based observations. Journal of Geophysical Research: Space Physics **126**(2) (2021) https://doi.org/10.1029/2020ja028368

Spogli, L., Alberti, T., Bagiacchi, P., Cafarella, L., Cesaroni, C., Cianchini, G., Coco, I., Di Mauro, D., Ghidoni, R., Giannattasio, F., Ippolito, A., Marcocci, C., Pezzopane, M., Pica, E., Pignalberi, A., Perrone, L., Romano, V., Sabbagh, D., Scotto, C., Spadoni, S., Tozzi, R., Viola, M.: The effects of the may 2024 mother's day superstorm over the mediterranean sector: from data to public communication. Annals of Geophysics **67**(2), 218 (2024) https://doi.org/10.4401/ag-9117

Tariku, Y.A.: Patterns of GPS-TEC variation over low-latitude regions (African sector) during the deep solar minimum (2008 to 2009) and solar maximum (2012 to 2013) phases. Earth, Planets and Space **67**(1) (2015) https://doi.org/10.1186/s40623-015-0206-2

Tariku, Y.A.: Assessment of Variability of the TEC in the Equatorial Anomaly Region with a Focus over Africa Using Rz and F10.7 as Input Drivers. The Astronomical Journal **160**(4), 185 (2020) https://doi.org/10.3847/1538-3881/abaf02

Tesema, F., Mesquita, R., Meriwether, J., Damtie, B., Nigussie, M., Makela, J., Fisher, D., Harding, B., Yizengaw, E., Sanders, S.: New results on equatorial thermospheric winds and temperatures from Ethiopia, Africa. Annales Geophysicae **35**(2), 333–344 (2017) https://doi.org/10.5194/angeo-35-333-2017

Tilahun, S., Asmare Tariku, Y.: Verification of ionospheric perturbation induced l-band frequency scintillation using hf/vhf bands over the african equatorial and low latitude region, ethiopia. Journal of Atmospheric and Solar-Terrestrial Physics **195**, 105135 (2019) https://doi.org/10.1016/j.jastp.2019.105135

Tornatore, V., Cesaroni, C., Pezzopane, M., Alizadeh, M.M., Schuh, H.: Performance evaluation of vtec gims for regional applications during different solar activity periods, using ring tec values. Remote Sensing **13**(8), 1470 (2021) https://doi.org/10.3390/rs13081470

Torr, M.R., Torr, D.G.: The seasonal behaviour of the f2-layer of the ionosphere. Journal of Atmospheric and Terrestrial Physics **35**(12), 2237–2251 (1973) https://doi.org/10.1016/0021-9169(73)90140-2

Tsunoda, R.T., Bubenik, D.M., Thampi, S.V., Yamamoto, M.: On large-scale wave structure and equatorial spread F without a post-sunset rise of the F layer . Geophysical Research Letters **37**(7), (2010) https://doi.org/10.1029/2009gl042357

Wernik, A.W., Secan, J.A., Fremouw, E.J.: Ionospheric irregularities and scintillation. Advances in Space Research **31**(4), 971–981 (2003) https://doi.org/10.1016/S0273-1177(02)00795-0

Wiens, R.H., Ledvina, B.M., Kintner, P.M., Afewerki, M., Mulugheta, Z.: Equatorial plasma bubbles in the ionosphere over eritrea: occurrence and drift speed. Annales Geophysicae **24**(5), 1443–1453 (2006) https://doi.org/10.5194/angeo-24-1443-2006

1009 Woodman, R.F.: Vertical drift velocities and east-west electric fields at the magnetic
1010 equator. Journal of Geophysical Research **75**(31), 6249–6259 (1970) https://doi.
1011 org/10.1029/ja075i031p06249

1012 Wu, C.C., Fry, C.D., Liu, J.Y., Liou, K., Tseng, C.L.: Annual TEC variation in the
1013 equatorial anomaly region during the solar minimum: September 1996-August 1997.
1014 Journal of Atmospheric and Solar-Terrestrial Physics **66**(3-4), 199–207 (2004) https:
1015 //doi.org/10.1016/j.jastp.2003.09.017

1016 Yamazaki, Y., Maute, A.: Sq and eej—a review on the daily variation of the geomag-
1017 netic field caused by ionospheric dynamo currents. Space Science Reviews **206**(1–4),
1018 299–405 (2017) https://doi.org/10.1007/s11214-016-0282-z

1019 Yeh, K.C., Liu, C.H.: Radio Wave Scintillations in the Ionosphere. Proceedings of the
1020 IEEE **70**(4), 324–360 (1982) https://doi.org/10.1109/PROC.1982.12313

1021 Yizengaw, E., Groves, K.M.: Longitudinal and seasonal variability of equatorial iono-
1022 spheric irregularities and electrodynamics. Space Weather **16**(8), 946–968 (2018)
1023 https://doi.org/10.1029/2018sw001980

1024 Yokoyama, T.: A review on the numerical simulation of equatorial plasma bubbles
1025 toward scintillation evaluation and forecasting. Progress in Earth and Planetary
1026 Science **4**(1) (2017) https://doi.org/10.1186/s40645-017-0153-6